Available online at www.sciencedirect.com
ScienceDirect
Journal of Solid State Chemistry 180 (2007) 3310–3316
JOURNAL OF SOLID STATE CHEMISTRY
www.elsevier.com/locate/jssc

Rietveld refinement and photoluminescent properties of a new blue-emitting material: Eu^{2+} activated $SrZnP_2O_7$

Jun-Lin Yuan[a,c], Xiao-Yan Zeng[b,c], Jing-Tai Zhao[a,*], Zhi-Jun Zhang[a,c], Hao-Hong Chen[a], Guo-Bin Zhang[d]

[a]*State Key Laboratory of High Performance Ceramics and Superfine Microstructure, Shanghai Institute of Ceramics, Chinese Academy of Sciences, Shanghai 200050, PR China*
[b]*Key Laboratory of Materials Physics, Institute of Solid State Physics, Chinese Academy of Science, Hefei 230031, PR China*
[c]*Graduate School of Chinese Academy of Sciences, Beijing, PR China*
[d]*NSRL, University of Science and Technology of China, Hefei 230027, PR China*

Received 29 May 2007; received in revised form 4 September 2007; accepted 16 September 2007
Available online 24 October 2007

Abstract

A new efficient blue phosphor, Eu^{2+} activated $SrZnP_2O_7$, has been synthesized at 1000 °C under reduced atmosphere and the crystal structure and photoluminescence properties have been investigated. The crystal structure of $SrZnP_2O_7$ was obtained via Rietveld refinement of powder X-ray diffraction (XRD) pattern. It was found that $SrZnP_2O_7$ crystallizes in space group of $P2_1/n$ (no. 14), $Z = 4$, and the unit cell dimensions are: $a = 5.30906(2)$ Å, $b = 8.21392(3)$ Å, $c = 12.73595(5)$ Å, $\beta = 90.1573(3)^\circ$, and $V = 555.390(3)$ Å^3. Under ultraviolet excitation (200–400 nm), efficient Eu^{2+} emission peaked at 420 nm was observed, of which the luminescent efficiency at the optimal concentration of Eu^{2+} (4 mol%) was estimated to be 96% as that of $BaMgAl_{10}O_{17}:Eu^{2+}$. Hence, the $SrZnP_2O_7:Eu^{2+}$ exhibit great potential as a phosphor in different applications, such as ultraviolet light emitting diode and photo-therapy lamps.

Keywords: $SrZnP_2O_7$; Eu^{2+} luminescence; Blue phosphor; Rietveld refinement

1. Introduction

Rare earth activated wide band gap luminescent materials are widely used in diverse applications, such as lamp phosphor, color display and X-ray imaging [1]. Among these luminescent materials, Eu activated phosphors have been studied intensely since Eu^{3+} is an ideal red-emitting activator and Eu^{2+} can emit photons in a wide energy range from UV to red depending on the nature of the host [2]. In the last decade, designing and researching new Eu^{2+} activated phosphors have been boosted by the development of light emitting diode (LED) lighting industry around the globe [3–5].

$A_2P_2O_7$ (A = Ca, Sr, Ba; Mg, Zn) is a large family of pyrophosphate compounds, which have been found to crystallize in two structural types that can be predicted from the ionic radius of A cation. When radius of A^{2+} is smaller than 0.97 Å (A = Mg, Zn), $A_2P_2O_7$ is of the thortveitite structure, in which $[P_2O_7]$ groups are in stagger configuration; and when the radius of A^{2+} is larger than 0.97 Å (A = Ca, Sr, Ba), the $[P_2O_7]$ groups are in eclipsed configuration [6]. The luminescent properties, especially the Eu^{2+}-doped diphosphates, such as $Ca_2P_2O_7:Eu^{2+}$, α-$Sr_2P_2O_7:Eu^{2+}$, $MgSrP_2O_7:Eu^{2+}$ and $MgBaP_2O_7:Eu^{2+}$ were found to be efficient phosphors in the violet–blue region [7]. By introducing optical inert ions into the lattice, such as Zn^{2+}, it is possible to tailor the luminescent properties. Among the alkali zinc diphosphates, $BaZnP_2O_7$ was found to crystallize in space group of $P\bar{1}$ (no. 2) with $Z = 2$ [8], whereas for both $CaZnP_2O_7$ and $SrZnP_2O_7$ there are only powder X-ray diffraction (XRD) patterns compiled in ICDD database (no. 53-0681 and no. 49-1026) and no detailed crystallographic data has been reported yet. Though the dielectric properties of $AZnP_2O_7$ (A = Ca, Sr) have been studied systematically [9–11], so far as we know,

*Corresponding author. Fax: +86 21 52413122.
E-mail address: jtzhao@mail.sic.ac.cn (J.-T. Zhao).

0022-4596/$ - see front matter © 2007 Elsevier Inc. All rights reserved.
doi:10.1016/j.jssc.2007.09.023

there is no report on the photoluminescence of Eu^{2+}-doped alkali earth zinc diphosphates, $A_{1-x}Eu_xZnP_2O_7$ (A = Ca, Sr, Ba). In this work, the crystal structure of $SrZnP_2O_7$ was obtained from Rietveld refinement, and the photoluminescent properties of $SrZnP_2O_7$:Eu^{2+} were reported for the first time. It was found that $SrZnP_2O_7$:Eu^{2+} is an efficient violet–blue emitting phosphor.

2. Experimental sections

2.1. Sample preparation

All the $Sr_{1-x}Eu_xZnP_2O_7$ (x = 0, 0.005, 0.01, 0.02, 0.03, 0.04, 0.05, 0.06) powder samples were prepared through solid-state reactions at high temperatures. The analytical pure starting materials, $SrCO_3$, ZnO, $(NH_4)_2HPO_4$ and Eu_2O_3 were weighed stoichiometrically, ground and mixed thoroughly in an agate mortar, fired in alumina crucibles at 400 °C for 1 h to remove volatile gas such as water and ammonia, then calcined at 900 °C for another 24 h. The Eu^{2+}-doped samples were obtained by a final heat treatment at 1000 °C for 4 h in a reducing atmosphere of H_2/Ar (volume ratio of 5/95). It was found that Eu^{3+} in the samples cannot be totally reduced when reduced at 900 °C, and the samples would melt when reduced at 1050 °C. All samples were purely white and non-hygroscopic.

2.2. XRD measurement and Rietveld refinement

The powder XRD pattern for Rietveld refinement was collected at ambient temperature on a HUBER Imaging Plate Guinier Camera G670[S] (Cu$K\alpha$1 radiation, λ = 1.54056 Å, germanium monochromator). The 2θ ranges of all the data sets are from 10° to 100° with a step of 0.005°, and the time of data collection is 8 h.

All calculations were carried out with *FullProf* program [12]. The Pseudo-Voigt peak profile function was used, and the background was approximated by linear interpolation between a set of background points with refinable heights. Due to the similar size of Zn^{2+} and Cr^{2+}, $SrCrP_2O_7$ (space group of $P2_1/n$, $Z = 4$) [13] was found to be the structure analog for $SrZnP_2O_7$, from which the atomic positions were used as the starting parameters in the Rietveld refinement. The observed, calculated and difference powder XRD patterns were shown in Fig. 1. The obtained reliability factors are: $R_p\% = 1.17$, $R_{wp}\% = 1.77$, $R_{exp}\% = 0.71$ and $\chi^2 = 6.21$, revealing the good quality of refinement. Moreover, the correctness of the refinement is indicated by checking the atom distances and angles (Table 2). For instance, the P–O distances are in the range of 1.471(4)–1.597(4) Å and the average P–O distance is 1.533 Å that is very close to 1.54 Å for P–O [14]. The Sr–O and Zn–O distances are normal as well.

2.3. Optical measurements

The vacuum ultraviolet (VUV) excitation and emission spectra were measured at the VUV spectroscopy experimental station on beam line U24 of the National Synchrotron Radiation Laboratory (NSRL), University of Science and Technology of China (USTC). The electron energy of the storage ring was 800 MeV and the beam current was about 150–250 mA with a lifetime of approximately 10 h. The synchrotron radiation was monochromatized through a Seya-Namioka monochromator and the signal was received by a Hamamatsu H5920-01 photomultiplier. The resolution of the instruments is about 0.2 nm. The relative VUV excitation intensities of the samples are corrected by dividing the measured excitation intensities of the samples with that of sodium salicylate in the same excitation conditions. Because the range of wavelength in the VUV–UV excitation spectra is 130–350 nm, the lower energy part of UV excitation spectra (350–410 nm) was recorded on a Shimadzu RF-5301 spectrofluorometer equipped with a 150 W xenon lamp as the excitation source. All of the excitation and emission spectra are recorded at room temperature.

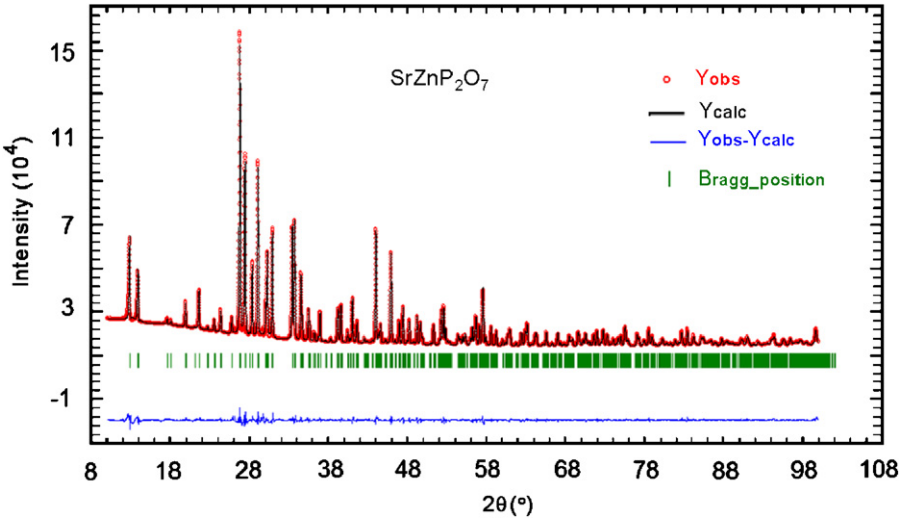

Fig. 1. Rietveld refinement of powder XRD pattern of undoped $SrZnP_2O_7$.

3. Crystal structure description

The unit cell dimensions obtained from Rietveld refinement are: $a = 5.30906(2)$ Å, $b = 8.21392(3)$ Å, $c = 12.73595(5)$ Å, $\beta = 90.1573(3)^\circ$ and $V = 555.390(3)$ Å^3, which match well with the values in ICDD no. 49-1026. The atomic positions were tabulated in Table 1, and the selected bond lengths and angles were listed in Table 2.

As shown in the projection of $SrZnP_2O_7$ view along the [1 0 0] and [0 1 0] axis (Fig. 2), [ZnO_5] pyramids and [P_2O_7] groups connect with each other to form a 3D-netwok by sharing the oxygen at the vertex of polyhedra, and Sr^{2+} ions locate at the dodecahedra formed in the Zn–P–O network. Different from another blue phosphor, α-$Sr_2P_2O_7$ (*Pnma* (no. 62), $Z = 4$), in which the [P_2O_7] groups are in eclipsed configuration [15], the [P_2O_7] groups in $SrZnP_2O_7$ are in a stagger configuration (Fig. 3c) since half of the cation sites in the pyrophosphate lattice are occupied by the smaller Zn^{2+} cations. Zn^{2+} coordinates with five oxygens with average Zn–O distance of 2.066 Å, and Sr^{2+} coordinates with eight oxygens with average Sr–O distance of 2.625 Å (Fig. 3 and Table 2). Each Sr^{2+} has two nearest neighboring Sr^{2+} ions along the [0 1 0] axis with Sr–Sr inter-cation distance of 4.191(1) Å, and two next nearest neighboring Sr^{2+} ions along the [1 0 0] axis with Sr–Sr inter-cation distance of 5.309(1) Å. Among the seven oxygen anions in each formula of $SrZnP_2O_7$, O_4 is the bridging oxygen in one [P_2O_7] group and each of the other six oxygens is the shared vertex of one [SrO_8] dodecahedron, one [ZnO_5] pyramid and one [PO_4] tetrahedron. The sites of dopants in the host are determined by their ionic radius. The radius of Eu^{3+}, Eu^{2+}, Sr^{2+} and Zn^{2+} is 1.07 Å (CN = 8), 1.25 Å (CN = 8), 1.26 Å (CN = 8) and 0.74 Å (CN = 6), respectively [16]. Consequently, the europium dopants (Eu^{3+} or Eu^{2+}) can more easily occupy the Sr^{2+} sites rather than the smaller Zn^{2+} sites.

4. Photoluminescent properties

Let us first examine the photoluminescent properties of Eu^{3+}-doped sample prior to the reduction treatment, which shows relatively weak orange–red emissions of Eu^{3+} under UV radiation. As shown in Fig. 4a, the excitation spectra is characterized by very weak host absorption band and broad charge transfer state (CTS) [2] band within 180–280 nm that peaked at 247 nm. And in the emission spectra (Fig. 4b), the intensity of magnetic-dipole transitions of $^5D_0$–$^7F_1$ (587 and 593 nm) is stronger than that of the electric-dipole transitions of $^5D_0$–$^7F_2$ (611 and 620 nm), which indicates that the Eu substituted Sr^{2+} site is basically centro-symmetric [1].

However, after the reduction heat treatment in H_2/Ar atmosphere at 1000 °C, narrow Eu^{3+} emission lines vanished completely and broad Eu^{2+} emission band dominated the spectra. As presented in Fig. 5, a strong Gaussian emission band was observed at 420 nm with

Table 2
Selected bond lengths (Å) and angles (°) in $SrZnP_2O_7$

Sr1					
O1	2.627(3)	O1–P1–O3	105.4(2)	O1–Sr1–O2	74.8(1)
O2	2.627(4)	O1–P1–O4	107.7 (2)	O1–Sr1–O3	53.7(1)
O3	2.723(3)	O1–P1–O5	116.2(2)	O1–Sr1–O5	78.8(1)
O3	2.549(3)	O3–P1–O4	107.0(2)	O1–Sr1–O6	151.2(1)
O5	2.501(3)	O3–P1–O5	113.9(2)	O1–Sr1–O7	68.1(1)
O5	2.527(3)			O2–Sr1–O3	64.0(1)
O6	2.692(3)	O2–P2–O4	106.1(2)	O2–Sr1–O5	79.0(1)
O7	2.755(3)	O2–P2–O6	111.0(2)	O2–Sr1–O6	76.5(1)
Zn1					
O1	2.034(4)	O2–P2–O7	111.0(2)		
O2	2.037(3)	O4–P2–O6	109.4(2)		
O3	2.173(4)	O4–P2–O7	102.2(2)		
O6	2.100(3)				
O7	1.988(4)	O7–Zn1–O1	108.6(1)		
P1					
O1	1.471(4)	O7–Zn1–O2	98.7(1)		
O3	1.553(4)	O7–Zn1–O3	79.3(1)		
O4	1.597(4)	O7–Zn1–O6	120.1(1)		
O5	1.521(4)	O1–Zn1–O3	87.8(1)		
P2					
O2	1.518(4)	O1–Zn1–O6	86.1(1)		
O4	1.578(3)	O2–Zn1–O3	84.6(1)		
O6	1.474(4)	O2–Zn1–O6	91.4(1)		
O7	1.552(3)				

Table 1
Atomic positions in the unit cell of $SrZnP_2O_7$ obtained from Rietveld refinement

Atom	Wyck.	Site symmetry	x/a	y/b	z/c	U [Å^2]
Sr1	4e	1	0.28706(13)	0.33960(6)	0.27904(5)	0.0077(2)
Zn1	4e	1	0.82887(17)	0.15179(11)	0.10540(6)	0.0093(3)
P1	4e	1	0.7497(3)	0.5344(2)	0.16429(12)	0.0039(5)
P2	4e	1	0.3183(3)	0.19912(18)	0.97944(12)	0.0029(5)
O1	4e	1	0.6681(7)	0.3642(5)	0.1527(2)	0.0021(11)
O2	4e	1	0.6753(7)	0.4040(4)	0.4004(3)	0.0054(12)
O3	4e	1	0.9540(6)	0.1169(4)	0.2664(3)	0.0054(12)
O4	4e	1	0.7648(7)	0.1180(3)	0.4488(3)	0.0037(11)
O5	4e	1	0.4824(6)	0.0604(4)	0.2966(3)	0.0025(12)
O6	4e	1	0.0912(6)	0.3327(4)	0.4737(2)	0.0029(11)
O7	4e	1	0.1974(7)	0.1868(4)	0.0900(2)	0.0025(12)

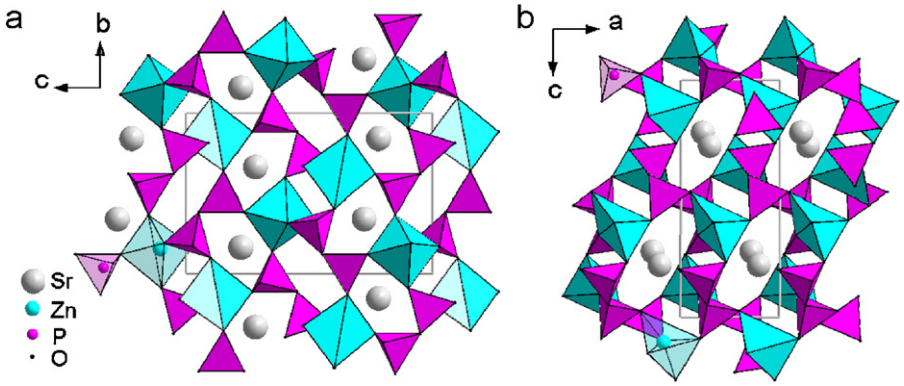

Fig. 2. Projection view of $SrZnP_2O_7$ from (a) *a*-axis and (b) *b*-axis.

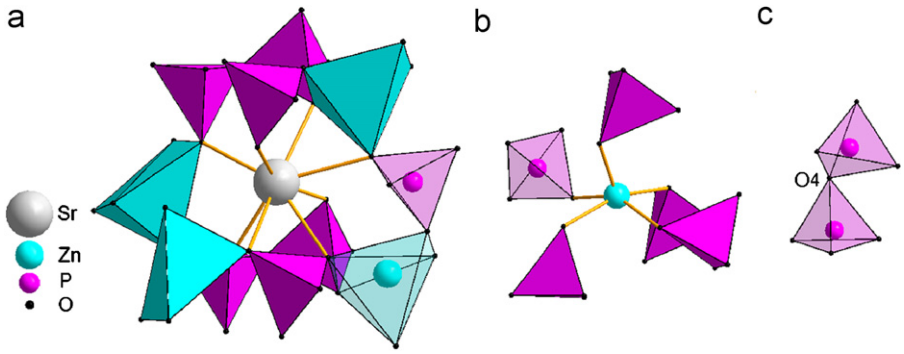

Fig. 3. The coordination environment of (a) Sr^{2+} and (b) Zn^{2+} ion in $SrZnP_2O_7$. (c) The connection between two $[PO_4]$ tetrahedra in the $[P_2O_7]$ group. The pink tetrahedra and cyan pyramid correspond to $[PO_4]$ and $[ZnO_5]$ groups, respectively.

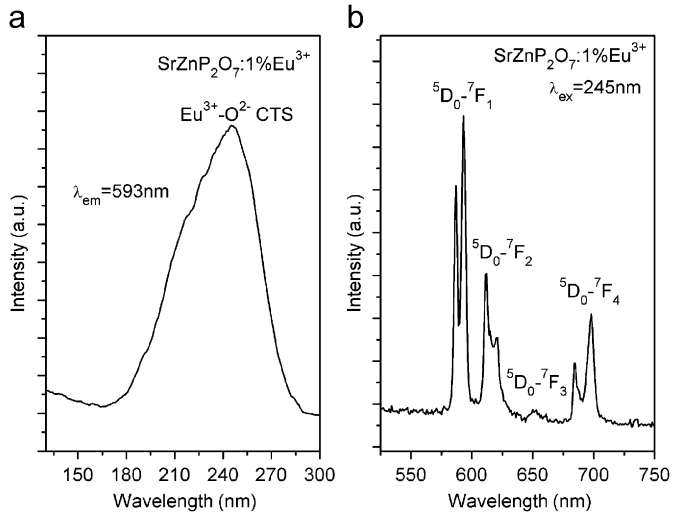

Fig. 4. VUV–UV excitation and emission spectra of $SrZnP_2O_7$:1% Eu^{3+} powder sample at room temperature.

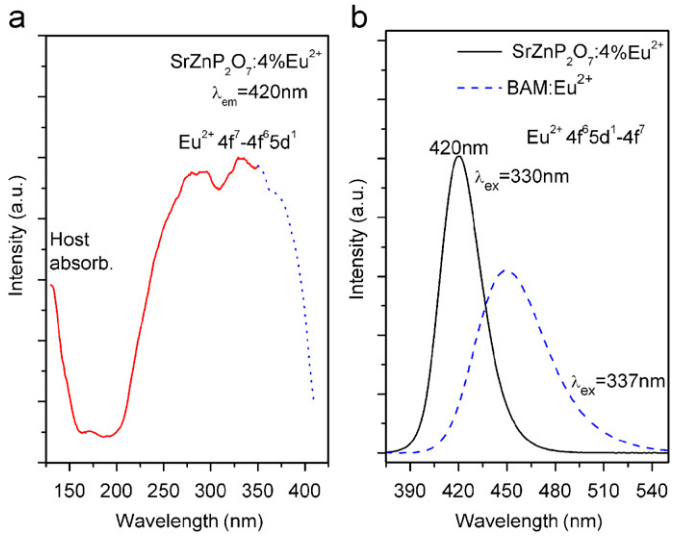

Fig. 5. (a) VUV–UV excitation spectra monitoring the strongest emission of $SrZnP_2O_7$:4% Eu^{2+} at 420 nm, in which the red solid curve was obtained at the VUV station of NSRL and the blue dot line was recorded using a Shimadzu RF-5301 spectrofluorophotometer. (b) UV-excited emission spectra of $SrZnP_2O_7$:4% Eu^{2+}, together with the emission spectra of BAM:Eu^{2+} measured under the same conditions as a reference.

FWHM of 30 nm, which could be assigned as the $4f^65d^1$–$4f^7$ parity-allowed transition of Eu^{2+} in $SrZnP_2O_7$. The excitation spectra consists of two parts: the host absorption band in the $\lambda < 160$ nm region that corresponds to the transition from valence band to conduction band and energy transfer from host to Eu^{2+} activators, and the broad band within 200–400 nm that corresponds to transition from the ground state $4f^7$ ($^8S_{7/2}$) to the excitation states $4f^65d^1$ of Eu^{2+}. As a result, the optical bandgap (E_g)

of the host was calculated to be 7.8 eV, which is very close to the intra-molecular absorption edge of $[PO_4]$ group [17]. The lowest $4f^6 5d^1$ absorption band of Eu^{2+} locates at 380 nm, from which the Stokes shift was calculated to be 2500 cm^{-1}.

The lowest $4f^6 5d^1$ absorption band of Eu^{2+} at 380 nm is 1925 cm^{-1} higher than the lowest $4f^6 5d^1$ absorption band of Eu^{2+} in α-$Sr_2P_2O_7$, of which the lowest absorption band locates at 410 nm and the main emission band locates at 420 nm [18]. The difference in the energy positions of the lowest $4f^6 5d^1$ band can be understood following Dorenbos's formula [2,19]:

$$D(3+, A) = \varepsilon_c + \frac{\varepsilon_{cfs}}{r(A)} - 1890\,cm^{-1}, \quad (1)$$

in which $D(3+, A)$ is the redshift of the lowest $5d$ level of Ce^{3+} in host A, centroid shift ε_c is the downward shift of the average energy of the $5d$ levels relative to that of free ion, crystal field splitting ε_{cfs} is the difference between the energy of the lowest and highest $5d$ level. ε_c is commonly associated with the nephelauxetic effect which is often attributed to the covalency between the $5d$ orbital and the p-orbitals of the anion, and ε_{cfs} is determined by the shape and size of the first anion coordination polyhedron. Due to the similarity in $5d$ levels among rare earth ions, this formula is also applicable for predicting $5d$ level positions of Eu^{2+} [2]. Comparing with α-$Sr_2P_2O_7$, in which Sr^{2+} ion is 9-fold coordinated and the average Sr–O distance is 2.700 Å [15], in $SrZnP_2O_7$ the 50% occupation of the cationic sites by Zn^{2+} leads to shrinkage of the lattice and the reduction of both coordination number of Sr^{2+} and the average Sr–O distance, which result in the increase of crystal field splitting (ε_{cfs}) at Sr^{2+} site. However, since Zn^{2+} directly connects with the oxygen at the vertex of $[SrO_8]$ dodecahedron, and the electronegativity value of Zn (1.65) is considerably greater than that of Sr (0.95) [20], the Sr–O bond in $SrZnP_2O_7$ is less covalent than that in α-$Sr_2P_2O_7$, leading to the reduction of centroid shift (ε_c) value. The reduction of ε_c preponderates over the increase of ε_{cfs}. Hence, the $D(Eu^{2+}, SrZnP_2O_7)$ is smaller than $D(Eu^{2+}$, α-$Sr_2P_2O_7)$, and the lowest Eu^{2+} $4f^6 5d^1$ absorption band in $SrZnP_2O_7$ is higher than that in ε-$Sr_2P_2O_7$.

The influence of the Eu^{2+} concentration on the luminescence was investigated and the optimum concentration of Eu^{2+} in $SrZnP_2O_7$ was determined. As shown in Fig. 6, when the concentration of Eu^{2+} increases, the intensity of Eu^{2+} increases steadily until reaching the optimal concentration of 4 mol% and a further increase in concentration leads to the decrease of Eu^{2+} emission intensity due to concentration quenching. As the Eu^{2+} concentration increases, the distance between the Eu^{2+} ions becomes smaller, leading to the higher probability of energy transfer among the Eu^{2+} ions. From Fig. 6, it is clear that 4 mol% is the critical concentration of Eu^{2+}, from which a rough estimation of the critical distance (R_c) for energy transfer can be made using the formula

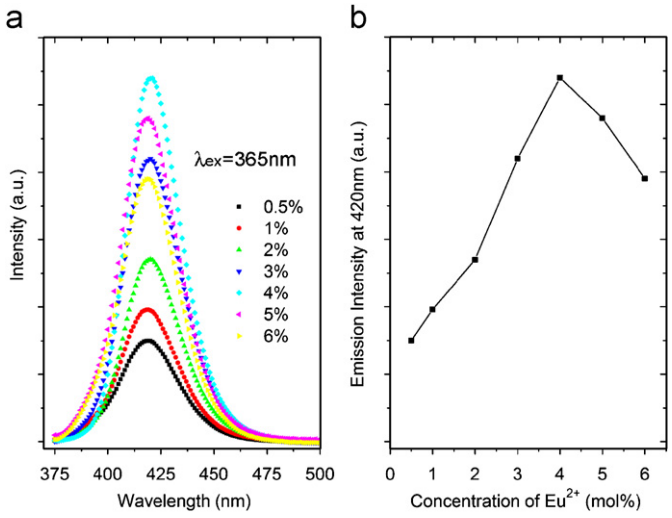

Fig. 6. (a) The emission spectra of $SrZnP_2O_7:Eu^{2+}$ with varying Eu concentration. (b) The Eu^{2+} concentration dependence of the emission intensity of $Sr_{1-x}Eu_xP_2O_7$ ($0<x<0.06$).

given by Blasse [21]:

$$R_c \approx 2\left[\frac{3V}{4\pi x_c Z}\right]^{1/3}, \quad (2)$$

in which V is the volume of the unit cell, x_c is the critical concentration of the activator ion, and Z is the number of formula units per unit cell. In the $SrZnP_2O_7:Eu^{2+}$ phosphor, Z equals 4, x_c and V are taken approximately as 0.04 and 555 $Å^3$, respectively, from which the critical distance of Eu^{2+} in $SrZnP_2O_7$, R_c, is estimated to be 19 Å, which is similar to the R_c value for Eu^{2+} centers in several oxide and nitride lattices [3,22–24].

Energy transfer is generally associated with exchange interaction, radiation re-absorption and multipolar interactions [25]. Since the overlap between wave functions of neighboring Eu^{2+} ions with such long distance is neglectable, the mechanism of exchange interaction plays little role in energy transfer between Eu^{2+} ions in $SrZnP_2O_7:Eu^{2+}$. Besides, it should be noted that there is little spectra overlap between excitation and emission spectra of $SrZnP_2O_7:Eu^{2+}$ (Fig. 5), and there is no variation in the position nor the profile of the Eu^{2+} emission spectra when Eu^{2+} concentration increases (Fig. 6a), which indicate that the energy transfer mechanism between Eu^{2+} ions should not be radiation re-absorption [26]. In addition, the fluorescent mechanism of Eu^{2+} is the parity-allowed electric-dipole transition of $4f^6 5d^1$–$4f^7$. As a result, the energy transfer should be dominated by electric multipolar interactions according to Dexter's theory [25].

In order to estimate the luminescent efficiency of $SrZnP_2O_7$:4% Eu^{2+} phosphor, a comparison was made with the standard commercial blue phosphor, $BaMgAl_{10}O_{17}:Eu^{2+}$ ($BAM:Eu^{2+}$) (Fig. 7), of which the emission spectrum was presented in Fig. 5b. Both phosphors were

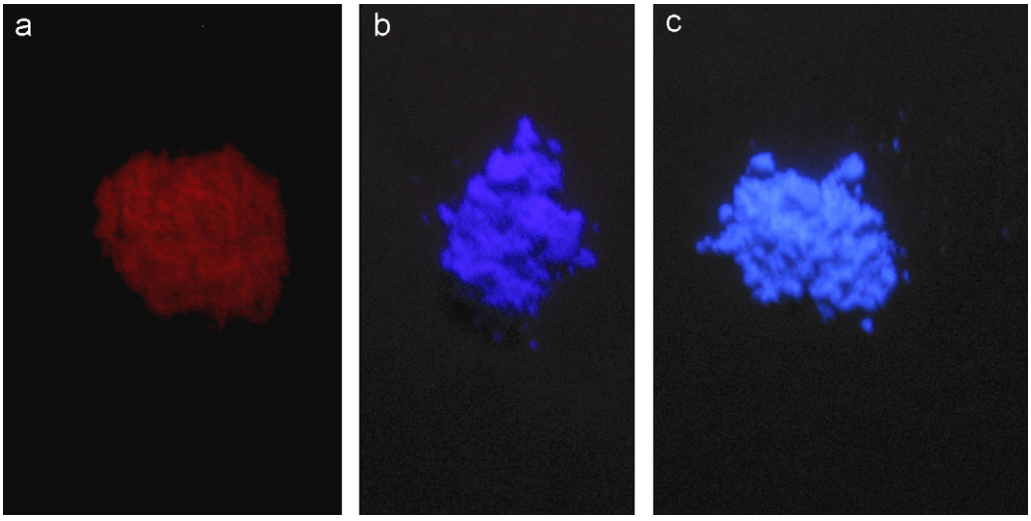

Fig. 7. Digital picture of the phosphors under the excitation of 254 nm of Hg lamp. (a) $SrZnP_2O_7$:4% Eu^{3+} (b) $SrZnP_2O_7$:4% Eu^{2+} and (c) commercial phosphor of $BaMgAl_{10}O_{17}:Eu^{2+}$ ($BAM:Eu^{2+}$).

measured under the same conditions and excited using their most efficient excitation wavelengths. By comparing the integration area of the emission curves, it was found that the quantum efficiency of $SrZnP_2O_7$:4%Eu^{2+} was 96% of that of $BaMgAl_{10}O_{17}:Eu^{2+}$, of which the quantum efficiency was regarded to be as high as 91% [27,28]. It is obvious that $SrZnP_2O_7:Eu^{2+}$ is a highly efficient UV-excited violet–blue emitting phosphor. $SrZnP_2O_7:Eu^{2+}$ can be efficiently excited by UV photons and there is little UV radiation in the emission, therefore $SrZnP_2O_7:Eu^{2+}$ is a candidate phosphor in UV-LED and lamps for photo-therapy [1].

5. Conclusion

An efficient violet–blue emitting phosphor, $SrZnP_2O_7:Eu^{2+}$ was reported in this work. $SrZnP_2O_7:Eu^{2+}$ was synthesized through solid-state reactions and reduced in H_2/Ar atmosphere at 1000 °C. By means of Rietveld refinement of powder XRD data, it was found that $SrZnP_2O_7$ crystallizes in space group of $P2_1/n$ (no. 14), $Z = 4$, and the unit cell parameters are: $a = 5.30906(2)$ Å, $b = 8.21392(3)$ Å, $c = 12.73595(5)$ Å, $\beta = 90.1573(3)^\circ$, and $V = 555.390(3)$ Å^3. $SrZnP_2O_7:Eu^{2+}$ can be efficiently excited by UV photons (200–400 nm) and emits strongly in the violet–blue region (420 nm, FWHM 30 nm), of which the quantum efficiency is estimated to be as high as 96% of standard commercial phosphor $BAM:Eu^{2+}$. $SrZnP_2O_7:Eu^{2+}$ is a potentially useful phosphor in UV-LED applications and lamps for photo-therapy.

Acknowledgments

This work was supported by the Key Project (50332050) from the NNSF of China, the Hundred Talents Program from the Chinese Academy of Sciences, Fund for Young Leading Researchers from Shanghai municipal government, and the "PHD Innovation Program 2006" by NSRL of ministry of education.

References

[1] G. Blasse, B.C. Grabmaier, Luminescent Materials, Springer, Berlin, 1994.
[2] P. Dorenbos, J. Lumin. 104 (2003) 239–260.
[3] Z.C. Wu, J.X. Shi, J. Wang, M.L. Gong, Q. Su, J. Solid State Chem. 179 (2006) 2356–2360.
[4] W.J. Yang, L. Luo, T.M. Chen, N.S. Wang, Chem. Mater. 17 (2005) 3883–3888.
[5] K.Y. Jung, H.W. Lee, H.K. Jung, Chem. Mater. 18 (2006) 2249–2255.
[6] I.D. Brown, C. Calvo, J. Solid State Chem. 1 (1970) 173.
[7] W.M. Yen, M.J. Weber, Inorganic Phosphors, CRC Press, Boca Raton, 2004.
[8] E.V. Murashova, Y.A. Velikodnyi, V.K. Trunov, Zhurnal Neorganicheskoi Khimii 36 (1991) 847–850.
[9] J.J. Bian, D.-W. Kim, K.S. Hong, Jpn. J. Appl. Phys. 43 (2004) 3521–3525.
[10] J.J. Bian, D.-W. Kim, K.S. Hong, Mater. Lett. 59 (2005) 257–260.
[11] J.J. Bian, D.-W. Kim, K.S. Hong, Mater. Res. Bull. 40 (2005) 2120–2129.
[12] J. Rodriguez-Carvajal, FullProf, July 2006, unpublished.
[13] A.A. El Belghiti, A. Boukhari, E.M. Holt, Acta Crystallogr. C 47 (1991) 473–477.
[14] M. Gabelica-Robett, M. Goreaud, P. Labbe, B. Raweau, J. Solid State Chem. 45 (1982) 389.
[15] J. Barbier, J.P. Echad, Acta Crystallogr. C 54 (1998) 2.
[16] A. Kelly, G.W. Groves, Crystallography and Crystal Defects, Addison-Wesley, Mass., 1970.
[17] S. Saito, K. Wada, R. Onaka, J. Phys. Soc. Jpn. 37 (1974) 711–715.
[18] G. Blasse, W.L. Wanmaker, J.W. ter Vrugt, J. Electrochem. Soc. 115 (1968) 673.
[19] P. Dorenbos, Phys. Rev. B 64 (2001) 125117.
[20] L.C. Allen, J. Am. Chem. Soc. 111 (1989) 9003–9014.
[21] G. Blasse, Philips Res. Rep. 24 (1969) 131.
[22] S.H.M. Poort, W.P. Blokpoel, G. Blasse, Chem. Mater. 7 (1995) 1547–1551.

[23] Y.Q. Li, G. de With, H.T. Hintzen, J. Alloy Compd. 385 (2004) 1–11.
[24] M. Kottaisamy, R. Jagannathan, P. Jeyagopal, R.P. Rao, R.L. Narayanan, J. Phys. D: Appl. Phys. 27 (1994) 2210.
[25] D.L. Dexter, J. Chem. Phys. 21 (1953) 836.
[26] F. Auzel, in: G. Liu, B. Jacquier (Eds.), Spectroscopic Properties of Rare Earths in Optical Materials, Springer, 2005, pp. 268–269.
[27] M. Zachau, J. Lumin. 72–74 (1997) 792–793.
[28] B. Moine, G. Bizarri, B. Varrel, J.-Y. Rivoire, Opt. Mater. 29 (2007) 1148–1152.